Laboratory Investigation (2014) 94, 1068–1082

Oxidative stress mediates the conversion of endothelial cells into myofibroblasts *via* a TGF-β1 and TGF-β2-dependent pathway

Ignacio Montorfano[1], Alvaro Becerra[1], Roberto Cerro[1], César Echeverría[1,2], Elizabeth Sáez[1], María Gabriela Morales[3], Ricardo Fernández[4], Claudio Cabello-Verrugio[3] and Felipe Simon[1,5]

During the pathogenesis of systemic inflammation, reactive oxygen species (ROS) circulate in the bloodstream and interact with endothelial cells (ECs), increasing intracellular oxidative stress. Although endothelial dysfunction is crucial in the pathogenesis of systemic inflammation, little is known about the effects of oxidative stress on endothelial dysfunction. Oxidative stress induces several functions, including cellular transformation. A singular process of cell conversion is tendothelial-to-mesenchymal transition, in which ECs become myofibroblasts, thus losing their endothelial properties and gaining fibrotic behavior. However, the participation of oxidative stress as an inductor of conversion of ECs into myofibroblasts is not known. Thus, we studied the role played by oxidative stress in this conversion and investigated the underlying mechanism. Our results show that oxidative stress induces conversion of ECs into myofibroblasts through decreasing the levels of endothelial markers and increasing those of fibrotic and ECM proteins. The underlying mechanism depends on the ALK5/Smad3/NF-κB pathway. Oxidative stress induces the expression and secretion of TGF-β1 and TGF-β2 and p38 MAPK phosphorylation. Downregulation of TGF-β1 and TGF-β2 by siRNA technology abolished the H_2O_2-induced conversion. To our knowledge, this is the first report showing that oxidative stress is able to induce conversion of ECs into myofibroblasts *via* TGF-β secretion, emerging as a source for oxidative stress-based vascular dysfunction. Thus, oxidative stress emerges as a decisive factor in inducing conversion of ECs into myofibroblasts through a TGF-β-dependent mechanism, changing the ECs protein expression profile, and converting normal ECs into pathological ones. This information will be useful in designing new and improved therapeutic strategies against oxidative stress-mediated systemic inflammatory diseases.

Laboratory Investigation (2014) **94,** 1068–1082; doi:10.1038/labinvest.2014.100; published online 28 July 2014

It is commonly accepted that the pathogenesis of inflammatory diseases underlies in the increment on oxidative stress. As a response for inflammation, immune system produces an uncontrolled response oversecreting mediators of inflammation including pro-inflammatory cytokines and cell-derived proteins.[1,2] The cell response generated by the mediators of inflammation is characterized by reactive oxygen species (ROS) overproduction, which increases in cellular oxidative stress.[1–3] Thus, changes in cellular oxidative stress are promoted by an increased ROS concentration through increases in ROS production and/or a decrease in the cellular clearance efficiency.[1,4] Low intracellular ROS concentrations are linked to normal cellular processes in healthy cells. In contrast, high ROS levels promote deleterious cellular effects.[2,4–8] The molecules that comprise the ROS family are oxidative molecules including the superoxide radical ($O_2^{\cdot -}$), hydrogen peroxide (H_2O_2), and the hydroxyl radical ($^{\cdot}OH$), among several others.[1,2]

During systemic inflammation, ROS circulate in the bloodstream and can interact directly with endothelial cells (ECs) in the inner wall of blood vessels,[1,9] which increases intracellular oxidative stress in ECs. Therefore, the ROS are

[1]Laboratorio de Fisiopatología Integrativa, Departamento de Ciencias Biologicas, Facultad de Ciencias Biologicas and Facultad de Medicina, Universidad Andres Bello, Santiago, Chile; [2]Laboratorio de Bionanotecnología, Universidad Bernardo O'Higgins, Santiago, Chile; [3]Laboratorio de Biología y Fisiopatología Molecular, Departamento de Ciencias Biologicas, Facultad de Ciencias Biologicas and Facultad de Medicina, Universidad Andres Bello, Santiago, Chile; [4]Laboratorio de Fisiología, Departamento de Ciencias Biologicas, Facultad de Ciencias Biologicas and Facultad de Medicina, Universidad Andres Bello, Santiago, Chile and [5]Millennium Institute on Immunology and Immunotherapy, Santiago, Chile
Correspondence: Dr F Simon, PhD, Departamento de Ciencias Biologicas, Facultad de Ciencias Biologicas and Facultad de Medicina, Universidad Andres Bello, Avenida Republica 252, 8370134 Santiago, Chile.
E-mail: fsimon@unab.cl

Received 2 April 2014; revised 4 June 2014; accepted 5 June 2014

generated within the endothelial monolayer and raise the intracellular level of oxidative stress in ECs.

An increase in oxidative stress causes cellular damage and cell transformation. Frequently, detrimental ROS-induced cellular effects are principally produced by protein and lipid modification, which alters their function and promotes abnormal cell processes.[4,10] Furthermore, ROS promote changes in the protein expression profile, which may modify cellular function.[11–15] High levels of oxidative stress induce cell death in several cell types. Moreover, it has been reported that increases in oxidative stress provoke cellular malignant transformation in the context of cancer.[16–18]

A well-known mechanism of cellular conversion is the epithelial-to-mesenchymal transition (EMT). Through the EMT, epithelial cells can change their phenotypic and functional features to become myofibroblasts to promote tissue fibrogenesis. Epithelial cells that are exposed to the most-used EMT inducer, tumor growth factor-beta (TGF-β), show a modification in their protein expression profile. Epithelial markers, such as E-cadherin, are downregulated, whereas fibroblast-specific genes, such as α-smooth muscle actin (α-SMA) and fibroblast-specific protein 1 (FSP-1), are upregulated. Furthermore, proteins that constitute the extracellular matrix (ECM), including fibronectin (FN), collagen type I and III, and vimentin are increased.[19–22]

TGF-β binds its plasma membrane receptor, activin receptor-like kinase 5 (ALK5), to activate it and subsequently elicit intracellular signaling.[23,24] Several proteins that are involved in TGF-β intracellular signaling include the canonical pathway of phosphorylation of the family of Smad proteins and non-canonical intracellular pathways, to perform the activation of nuclear factor-kappa B (NF-κB).[24–28] Specifically, the Smad3 protein emerges as a pro-fibrotic member of the Smad protein family because its phosphorylation promotes the progression of fibrosis.[29,30]

It has been reported that oxidative stress induces the EMT. Human epidermal keratinocytes exposed to H_2O_2 showed protein expression that was consistent with the EMT,[31] and similar results were founded in renal tubular epithelial cells.[32] In the same way, chromium-induced EMT is dependent on intracellular ROS in lung epithelial cells.[33]

A specialized EMT process is the endothelial-to-mesenchymal transition (EndMT). By means of the EndMT, ECs become myofibroblasts. Similarly, ECs exposed to TGF-β exhibit a decrease in the levels of the endothelial markers CD31 and VE-cadherin, whereas the fibroblast-specific genes α-SMA and FSP-1 are increased. Furthermore, the levels of proteins that form the ECM, such as FN and collagen type III, are greatly increased.[34,35]

In addition of changes in expression proteins, some aspects of ECs functionality are also modified once EndMT is established. Concordantly with the loss of VE-cadherin and CD-31 expression, ECs undergoing EndMT lose their cell-to-cell connection, suggesting that the endothelium loses its capacity to function as a selectively permeable barrier promoting increased filtration from the intravascular lumen to the interstitial fluid. Moreover, normal ECs exhibit a round, short-spindled morphology with a cobblestone appearance; thus, the endothelium is a perfect monolayer, which allows its function as selectively permeable barrier. However, by means of EndMT, a fibrotic-like spindle-shaped phenotype with non-connected cells is observed along with α-SMA and FSP-1 overexpression, which alters the cytoskeletal organization.[34–43] Furthermore, acquisition of ECM proteins such as fibronectin and collagen type III is a prominent functional feature of myofibroblasts that changes endothelial functionality. Healthy ECs secrete collagen type IV and low amounts of fibronectin, whereas collagen type I and type III are virtually absent, appearing only after fibrosis has been established and affecting normal endothelial function. The increase in ECM proteins during EndMT alters EC function because it affects the interaction between ligands and membrane receptors, protein turnover, and protein internalization.[34,36,37,41–47] In addition, increased cell migration is a major distinctive feature of myofibroblasts. Because EndMT is a cellular mechanism for the conversion of polarized ECs into motile mesenchymal cells, this process is also characterized by the acquisition of migratory features.[34,48,49] Therefore, through EndMT, ECs disaggregate from the vascular monolayer to migrate into the adjacent tissue.[34,48,49] Recently, we and others have reported that ECs exposed to EndMT inducers, such as endotoxins and oxidative stress, are able to induce increased endothelial migration similar to that observed in myofibroblasts.[50–52]

However, the participation of oxidative stress as an inductor of conversion of ECs into myofibroblasts and the underlying mechanism are not known.

Herein, we investigated the role played by oxidative stress in the conversion of ECs into myofibroblasts and the underlying mechanism.

We demonstrate that H_2O_2 induces conversion of ECs into myofibroblasts through decreasing the expression of endothelial markers and increasing the levels of fibrotic and ECM proteins. The underlying mechanism depends on ALK5 expression, Smad3 activation, and the intracellular NF-κB activity pathway. Furthermore, H_2O_2 induces the expression and secretion of TGF-β1 and TGF-β2 and the phosphorylation of p38 MAPK. Finally, we demonstrated that downregulation of TGF-β1 and TGF-β2 by siRNA technology abolished the H_2O_2-induced conversion of ECs into myofibroblasts.

These findings are useful for understanding the mechanisms involved in the oxidative stress-induced endothelial dysfunction that is observed during vascular inflammation.

MATERIALS AND METHODS

Details of all procedures are provided in Supplementary Information.

Primary Cell Culture

Human umbilical vein endothelial cells (HUVECs) were isolated by collagenase (0.25 mg/ml) digestion from freshly

obtained umbilical cord veins from normal pregnancies, after patient's informed consent. The investigation conforms to the principles outlined in the Declaration of Helsinki. The Commission of Bioethics and Biosafety of Universidad Andres Bello also approved all experimental protocols. Cells were grown in gelatin-coated dishes at 37 °C in a 5%:95% CO_2:air atmosphere in medium 199 (Sigma, MO), containing 100 μg/ml endothelial cell growth supplement (ECGS) (Sigma), 100 μg/ml heparin, 5 mM D-glucose, 3.2 mM L-glutamine, 10% fetal bovine serum (FBS) (GIBCO, NY), and 50 U/ml penicillin-streptomycin (Sigma). HUVECs were used between the third and fifth *in vitro* passage and always before the tenth day in culture, and 25–30 different batches of HUVECs were used.

Small Interfering RNA and Transfections

SiGENOME SMARTpool siRNA (four separated siRNAs per each human ALK5, TGF-β1 or TGF-β2 transcript) was purchased from Dharmacon (Lafayette, CO). The following siRNA was used: siRNA against human ALK5 (siALK5), siRNA against human TGF-β1 (siTGFβ1), siRNA against human TGF-β2 (siTGFβ2), and non-targeting siRNA (siCTRL) used as a control. In brief, HUVEC was plated overnight in 6-well plate and then transfected with 5 nM siRNA using the DharmaFECT 4 transfection reagent (Dharmacon) used according to the manufacturer's protocols in serum-free medium for 24 h. After 48–72 transfection, experiments were performed.

RNA Isolation and Quantitative Real-Time PCR

QPCR experiments were performed to measure TGF-β1 and TGF-β2 mRNA levels in HUVECs. Total RNA was extracted with Trizol according to the manufacturer's protocol (Invitrogen, Carlsbad, CA). DNAse I-treated RNA was used for reverse transcription using the Super Script II Kit (Invitrogen). Equal amounts of RNA were used as templates in each reaction. QPCR was performed using the SYBR Green PCR Master Mix (AB Applied Biosystems, Foster City, CA). All reactions were performed in triplicate on an Eco Real-Time PCR System (Illumina, USA). Data are presented as relative mRNA levels of the gene of interest normalized to relative levels of 28S mRNA.

Western Blot Procedures

Cells were lysed in cold lysis buffer, and then proteins were extracted. Supernatants were collected and stored in the same lysis buffer. Protein extract and supernatant were subjected to SDS-PAGE and resolved proteins were transferred onto a nitrocellulose or PVDF membrane. The blocked membrane was incubated with the appropriate primary antibody, washed twice, and incubated with a secondary antibody. Bands were detected using a peroxidase-conjugated IgG antibody and visualized by enhanced chemiluminescence (Thermo Scientific, USA). Tubulin was used as a loading control. Images were acquired using Fotodyne FOTO/Analyst Luminary Workstations Systems (Fotodyne, Inc., Hartland, WI). Protein content was determined by densitometric scanning of immunoreactive bands and intensity values were obtained by densitometry of individual bands normalized against control. For a detailed list of antibodies used, see Supplementary Table S1.

Fluorescent Immunocytochemistry

ECs were washed twice with PBS and fixed. The cells were subsequently washed again and incubated with the primary antibodies. Then, cells were washed twice and incubated with the secondary antibodies. Samples were mounted with ProLong Gold antifade mounting medium with DAPI (Invitrogen). For a detailed list of antibodies used, see Supplementary Table S2.

Reagents

H_2O_2, buffers, and salts were purchased from Merck Biosciences (Darmstadt). Smad3-specific inhibitor, SIS3, the NF-κB-specific inhibitor, IKK-16, and the ALK5-specific inhibitor, SB431542, were purchased from Tocris (Ellisville, MO, USA).

Data Analysis

All results are presented as the means ± s.d. ANOVA followed by the Dunn's *post hoc* tests were used and considered as significant at $P<0.05$.

RESULTS

H_2O_2 Induces the Conversion of ECs into Myofibroblasts

To test whether oxidative stress is able to induce the conversion of ECs into myofibroblasts, ECs were exposed to several concentrations of the oxidant agent H_2O_2, and endothelial and fibrotic characteristics were measured. ECs exposed to H_2O_2 exhibited a decrease in the levels of the endothelial proteins VE-cadherin (Figure 1a and b) and CD31 (Figure 1c and d) at every H_2O_2 concentration that was tested. Furthermore, consistent with the establishment of a fibrotic process, ECs challenged with H_2O_2 showed an increase in the fibrotic markers α-SMA (Figure 1e and f) and FSP-1 (Figure 1g and h) at every H_2O_2 dose that was tested.

We also investigated the effect of oxidative stress on the cellular localization and distribution of endothelial and fibrotic proteins. To that end, we performed immunocytochemistry experiments. ECs in the absence of H_2O_2 showed VE-cadherin labeling that was localized predominantly to the plasma membrane (Figure 2a and e). Similarly, characteristic CD31 labeling was also detected at the plasma membrane (Figure 2i and m). In contrast, the expression of the fibrotic marker FSP-1 was virtually undetectable (Figure 2a and e), while α-SMA was weakly expressed (Figure 2i and m). In the absence of H_2O_2, ECs showed their normal round shape, short-spindle morphology with a cobblestone appearance. However, ECs exposed to H_2O_2 showed a decrease in the endothelial proteins VE-cadherin (Figure 2b–d and f–h) and

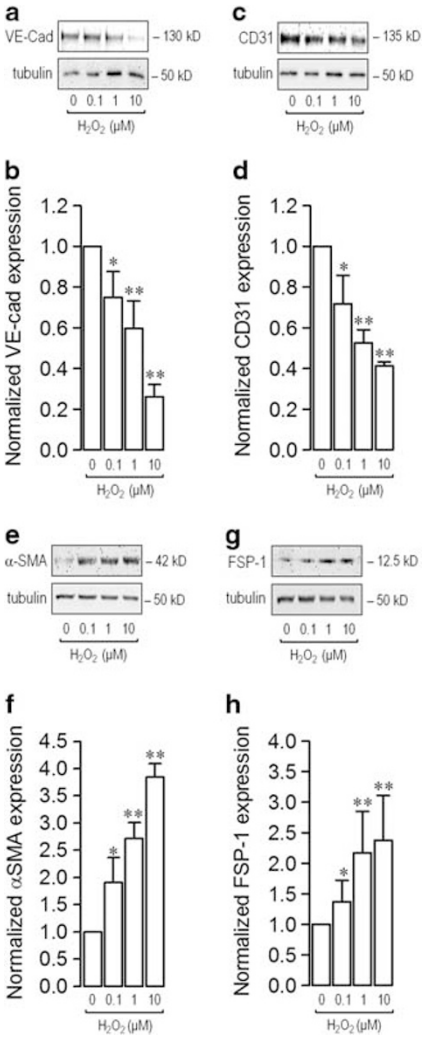

Figure 1 H_2O_2-induced changes in endothelial and fibrotic markers expression. (**a**–**h**) ECs were exposed to H_2O_2 for 72 h and protein expression was analyzed. (**a**, **c**, **e**, and **g**) Representative images from western blot experiments performed for detection of endothelial markers VE-cadherin (VE-cad) (**a**) and CD31 (**c**), and fibrotic markers α-SMA (**e**) and FSP-1 (**g**). (**b**, **d**, **f**, and **h**) Densitometric analyses of the experiments shown in (**a**, **c**, **e**, and **g**), respectively. Protein levels were normalized against tubulin and data are expressed relative to the untreated condition (0 μM H_2O_2). Statistical differences were assessed by a one-way analysis of variance (ANOVA) (Kruskal–Wallis) followed by Dunn's post hoc test. *: $P<0.05$ and **: $P<0.01$ against the untreated condition. Graph bars show the mean ± s.d. ($N=3$–5).

CD31 (Figure 2j–l and n–p). Furthermore, H_2O_2 exposure induced an increase in the fibrotic markers FSP-1 (Figure 2b–d and f–h) and α-SMA (Figure 2j–l and n–p). In the presence of H_2O_2, ECs exhibited a spindle-shaped, fibroblast-like phenotype, in which the monolayer distribution and the cell-to-cell connections were partially lost.

One of the major features of fibrosis development is the overproduction of ECM proteins.[6,53] Thus, we were prompted to measure the expression of the ECM proteins fibronectin and collagen type III and founded that both were increased in H_2O_2-treated ECs (Figure 3). ECs in the presence of several doses of H_2O_2 exhibited increased fibronectin (Figure 3a and b) and collagen type III (Figure 3c and d) at every H_2O_2 concentration that was tested.

Next, we evaluated the role of the oxidant H_2O_2 in the cellular localization and distribution of ECM proteins. As we showed before, ECs in the absence of H_2O_2 showed VE-cadherin (Figure 4a and e) and CD31 (Figure 4i and m) labeling that was localized mainly at the plasma membrane. On the contrary, the expression of the ECM protein fibronectin was slightly detected (Figure 4a, e, i, and m). However, H_2O_2-treated ECs showed a decrease in the detection of the endothelial proteins VE-cadherin (Figure 4b–d and f–h) and CD31 (Figure 4j–l and n–p). In addition, exposure to the oxidant induced an increase in fibronectin (Figure 4b–d, f–h, j–l, and n–p), which was observed as a net of fibrils surrounding the cells.

To demonstrate that our findings were obtained from a culture of human ECs without contamination from fibroblast-like cells, we carried out an exhaustive inspection of the EC culture.[37] To that end, we used the specific endothelial marker VE-cadherin and the specific fibrotic protein, FSP-1. We found that >99% of cells in the EC culture were positive for VE-cadherin, whereas those expressing FSP-1 were not detected. This quantification demonstrated that the primary human EC culture was highly enriched in ECs (Supplementary Figure S1).

H_2O_2-Induced Conversion of ECs into Myofibroblasts is Dependent on ALK5 Expression

As was previously mentioned, TGF-β is the most well-studied EndMT inducer. TGF-β binds to TβRII, which recruits the TβRI, ALK5.[23,24] Considering this evidence, we investigated whether ALK5 expression was involved in the H_2O_2-induced conversion of ECs into myofibroblasts. To that end, we performed experiments using a molecular biology strategy for ALK5 expression knockdown. To demonstrate the participation of ALK5 in H_2O_2-induced conversion of ECs into myofibroblasts, ECs were transfected with a specific small interference RNA (siRNA) against the human isoform of ALK5 (siALK5). The siRNA efficiency of ALK5 expression knockdown was >90% (Supplementary Figure S2).

ECs exposed to H_2O_2 and transfected with a non-targeting sequence siRNA were used as a control (siCTRL), and these cells showed a decrease in the protein level of VE-cadherin (Figure 5a and b) and an increase in the protein levels of α-SMA (Figure 5c and d) and the ECM protein fibronectin (Figure 5e and f), which were similar results to those observed in non-transfected, wild-type ECs (Figures 1 and 3). Additionally, ECs transfected with siCTRL in the absence of the oxidant did not show any change in the protein level of VE-cadherin, α-SMA, or fibronectin compared with non-transfected cells (not shown). In contrast, H_2O_2-treated ECs transfected with siALK5 did not show any decrease in the

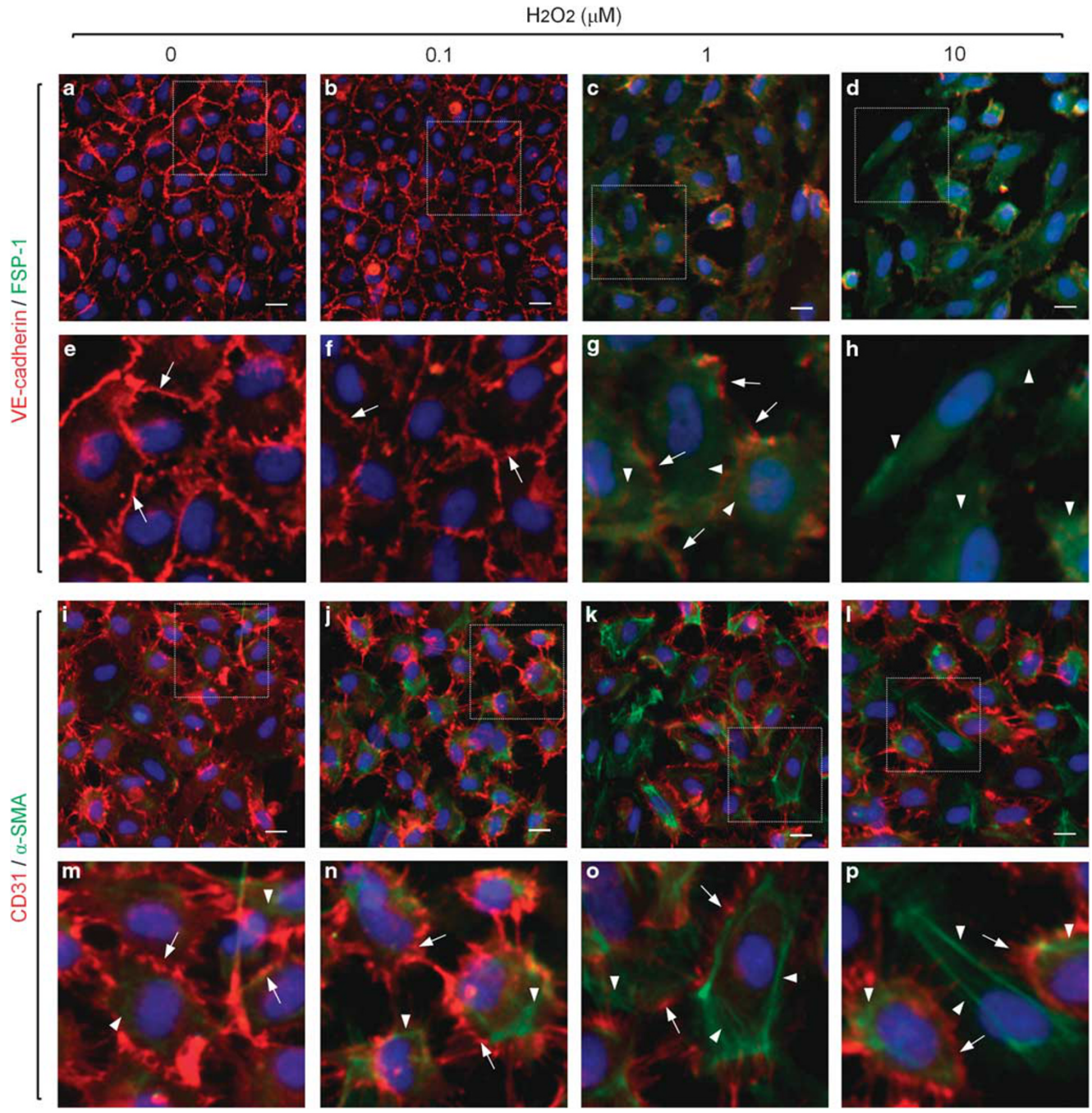

Figure 2 Cellular distribution of endothelial and fibrotic markers involved in H_2O_2-induced conversion of ECs into myofibroblasts. (**a**–**p**) Representative images from ECs in the absence of H_2O_2 (0 μM H_2O_2) (**a**, **e**, **i**, and **m**) or in the presence of 0.1 μM H_2O_2 (**b**, **f**, **j**, and **n**), 1 μM H_2O_2 (**c**, **g**, **k**, and **o**), and 10 μM H_2O_2 (**d**, **h**, **l**, and **p**) for 72 h. VE-cadherin or CD31 (red), and FSP-1 or α-SMA (green) were detected. The box depicted in (**a**-**d** and **i**-**l**) indicates the magnification shown in (**e**–**h** and **m**–**p**), respectively. Arrows indicate VE-Cadherin (**e**–**h**) or CD31 (**m**–**p**) labeling at the plasma membrane, whereas arrowheads indicate FSP-1 (**g**, **h**) or α-SMA (**m**–**p**) staining. Nuclei were stained using DAPI. Bar scale represents 10 μm ($N = 3$).

protein level of VE-cadherin (Figure 5a and b). Moreover, siALK5 transfection prevented the increase in the protein levels of α-SMA (Figure 5c and d) and the ECM protein fibronectin (Figure 5e and f). These results suggest that ALK5 expression is critically involved in H_2O_2-induced conversion of ECs into myofibroblasts.

H_2O_2-Induced Conversion of ECs into Myofibroblasts is Dependent on Smad3 Activation

It is well known that ALK5 phosphorylates the Smad protein family through the canonical signaling pathway to regulate gene transcription and exert fibrotic effects. Specifically, Smad3 phosphorylation has been linked to the fibrotic

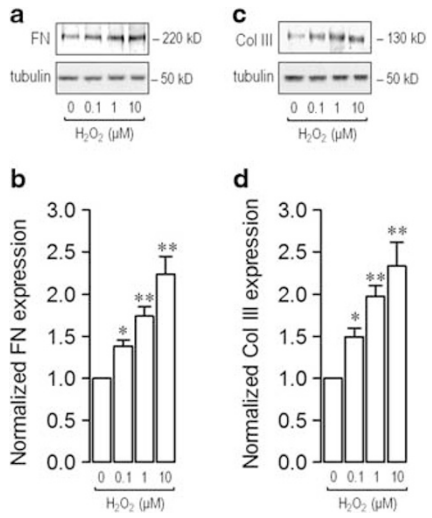

Figure 3 H_2O_2-induced changes in ECM proteins expression. (**a**–**d**) ECs were exposed to H_2O_2 for 72 h and protein expression was analyzed. (**a**, **c**) Representative images from western blot experiments performed for detection of the ECM proteins fibronectin (FN) (**a**) and collagen type III (Col III) (**c**). (**b** and **d**) Densitometric analyses of the experiments shown in (**a** and **c**), respectively. Protein levels were normalized against tubulin and data are expressed relative to the untreated condition (0 μM H_2O_2). Statistical differences were assessed by a one-way analysis of variance (ANOVA) (Kruskal–Wallis) followed by Dunn's *post hoc* test. *: $P<0.05$ and **: $P<0.01$ against the untreated condition. Graph bars show the mean ± s.d. ($N=3$–5).

process.[23,24] Thus, we addressed the question of whether Smad3 activation participates in the H_2O_2-induced conversion of ECs into myofibroblasts. To that purpose, we used the specific inhibitor of Smad3, SIS3.[54] To demonstrate that SIS3 was efficient to inhibit the activation of smad3 through translocation to nucleus, protein extracts from the cytosol (CF) and nuclear (NF) fractions were obtained from ECs exposed to the smad pathway inducer TGF-β1 incubated with or without SIS3. Results showed that in TGF-β1-treated EC, smad3 was detected predominantly in the NF that in the CF, suggesting nuclear translocation. However, in TGF-β1-treated EC with SIS3, smad3 was detected mainly in the CF, indicating that SIS3 inhibited the smad3 nuclear translocation (Figure 6a–d). Our results showed that ECs exposed to H_2O_2 in the presence of SIS3 failed to decrease their levels of the endothelial marker VE-cadherin (Figure 6e and f). In line with this finding, SIS3 treatment inhibited the increase in the fibrotic proteins α-SMA (Figure 6g and h) and fibronectin (Figure 6i and j). These results suggest that H_2O_2-induced conversion of ECs into myofibroblasts is dependent on Smad3 phosphorylation.

H_2O_2-Induced Conversion of ECs into Myofibroblasts is Dependent on NF-κB Activation

It has been reported that ALK5 activation is able to induce NF-κB activation to trigger gene expression through an intracellular signaling pathway.[25,26] Hence, we assessed whether NF-κB participates in the H_2O_2-induced conversion of ECs into myofibroblasts. To test this, we used the specific NF-κB inhibitor, IKK-16, which is a selective inhibitor of IκB kinase (IKK). NF-κB remains in the cytosol associated with IκB. When NF-κB is activated, IKK phosphorylates IκB triggering its degradation *via* proteasome, releasing NF-κB which can now enter the nucleus and regulate gene expression. To demonstrate that IKK-16 was able to inhibit NF-κB activation, ECs were exposed to the well-known NF-κB activator, endotoxin, in the presence or absence of IKK-16, and CF and NF were extracted. Endotoxin-treated EC incubated with IKK-16 abolished the NF-κB translocation to the nucleus (Figure 7a–d), suggesting that IKK-16 inhibited NF-κB translocation. H_2O_2-treated ECs in the presence of IKK-16 did not show any decrease in the endothelial marker VE-cadherin (Figure 7e and f). Furthermore, IKK-16 incubation inhibited the increase in the protein level of the fibrotic marker α-SMA (Figure 7g and h), as well as in the ECM protein fibronectin (Figure 7i and j). These results suggest that NF-κB activation is involved in the H_2O_2-induced conversion of ECs into myofibroblasts.

H_2O_2 Induces TGF-β1 and TGF-β2 Expression

Considering the dependence of H_2O_2-induced conversion of ECs into myofibroblasts on ALK5 expression, we were prompted to investigate whether H_2O_2 induced the production of the ligand of ALK5, TGF-β. Given that two isoforms of TGF-β, TGF-β1 and TGF-β2, have been implicated in the EndMT,[19,35,40] we determined the mRNA expression of TGF-β1 and TGF-β2 that was induced by H_2O_2. ECs exposed to H_2O_2 for 24 or 72 h showed an increase in mRNA expression of TGF-β1 (Figure 8a and b) and TGF-β2 (Figure 8c and d). In agreement with the changes in mRNA expression, supernatants of H_2O_2-treated ECs showed an increase in the protein level of TGF-β1 (Figure 8e and f) and TGF-β2 (Figure 8g and h).

Furthermore, we studied whether NF-κB activation by H_2O_2 was dependent on TGF-β pathway. To that end, we used SB431542 which is a specific inhibitor of the TGF-β receptor, ALK5. Thus, using the inhibitor of ALK5, SB431542, the TGF-β signaling is abolished. Results showed that H_2O_2-treated ECs without SB431542, NF-κB p65 was detected predominantly in the NF, suggesting nuclear translocation. Whereas, in H_2O_2-treated ECs with SB431542, NF-κB p65 detected in the NF was partially but significantly decreased. These results suggest that TGF-β pathway participates in the H_2O_2-induced NF-κB activation (Figure 8i-l).

Taking into consideration that TGF-β expression is dependent on p38 MAPK phosphorylation,[6,24] we studied whether H_2O_2 induces the increased phosphorylation of p38 MAPK. H_2O_2 exposure induced p38 MAPK phosphorylation showing a peak at 1 h after challenge (Supplementary Figure S3).

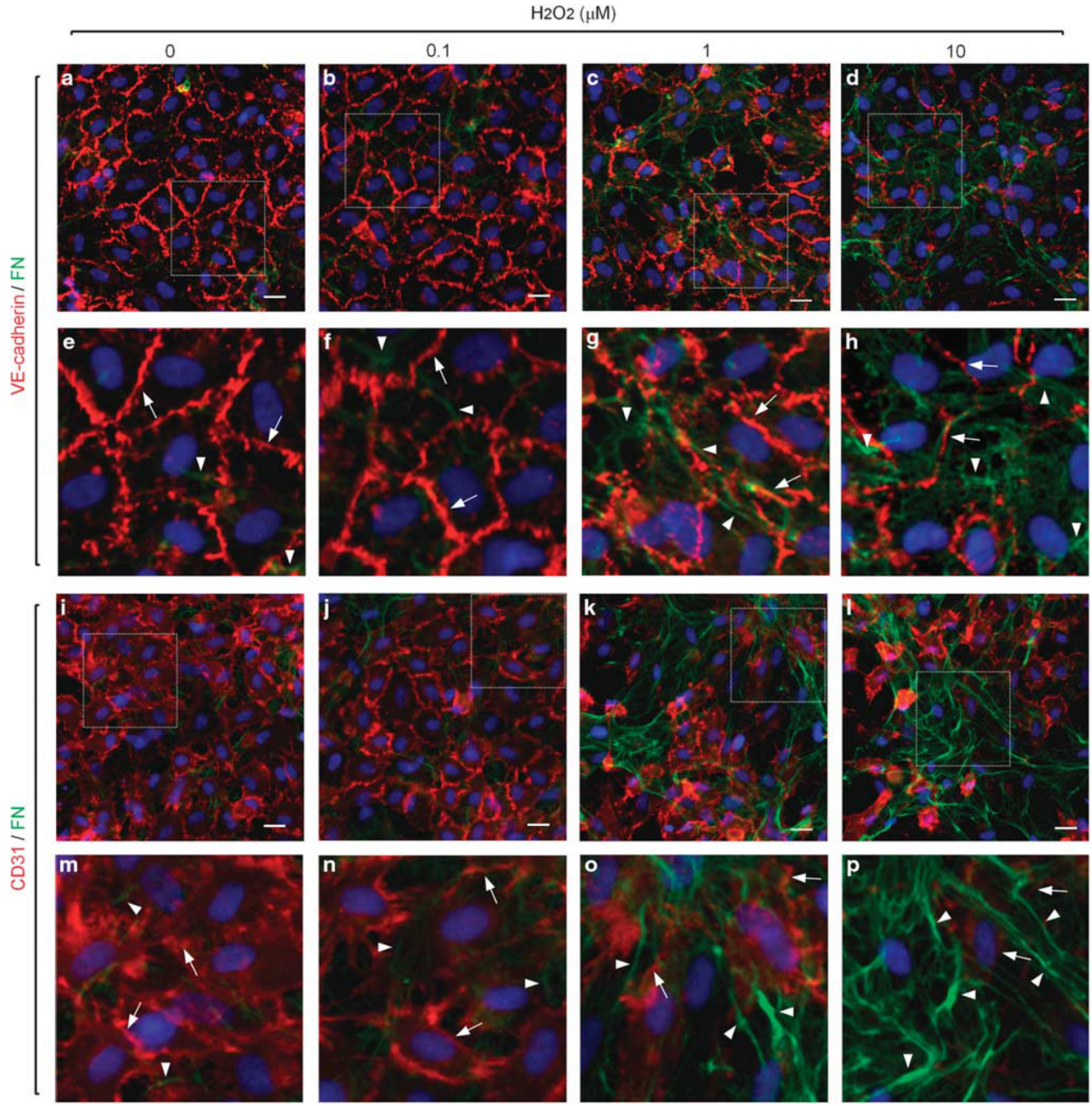

Figure 4 Cellular distribution of ECM proteins involved in H_2O_2-induced conversion of ECs into myofibroblasts. (**a**–**p**) Representative images from ECs in the absence of H_2O_2 (0 μM H_2O_2) (**a**, **e**, **i**, and **m**) or in the presence of 0.1 μM H_2O_2 (**b**, **f**, **j**, and **n**), 1 μM H_2O_2 (**c**, **g**, **k**, and **o**), and 10 μM H_2O_2 (**d**, **h**, **l**, and **p**) for 72 h. VE-cadherin or CD31 (red), and FN (green) were detected. The box depicted in (**a**–**d** and **i**–**l**) indicates the magnification shown in (**e**–**h** and **m**–**p**), respectively. Arrows indicate VE-Cadherin (**e**–**h**) or CD31 (**m**–**p**) labeling at the plasma membrane, whereas arrowheads indicate FN (**e**–**h** and **m**–**p**) staining. Nuclei were stained using DAPI. Bar scale represents 10 μm ($N = 3$).

H_2O_2-Induced Conversion of ECs into Myofibroblasts is Dependent on the Expression of TGF-β1 and TGF-β2

Taking into account that H_2O_2 induces the expression of TGF-β1 and TGF-β2, we tested whether the expression of these cytokines is necessary for the conversion of ECs into myofibroblasts induced by the oxidant. To that end, we used two specific siRNAs against each TGF-β isoform, TGF-β1 and TGF-β2. In addition, we used a non-targeting siRNA as a control (siCTRL). First, we tested whether the siRNAs were specific in the inhibition of TGF-β1 and TGF-β2. The siRNA

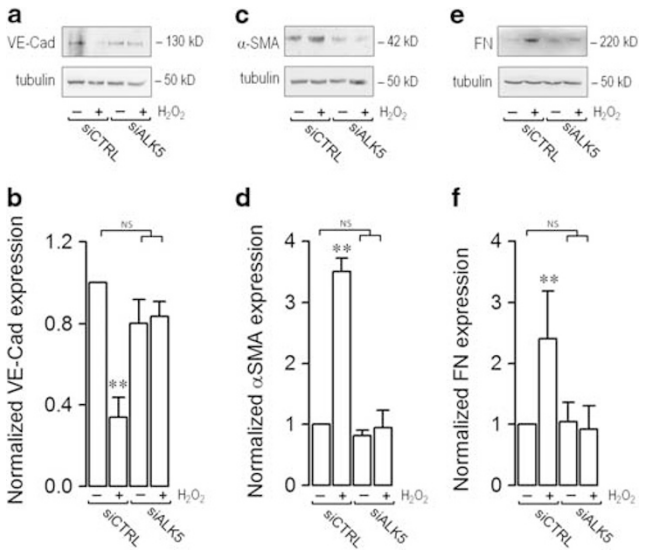

Figure 5 Changes in protein expression during H_2O_2-induced conversion of ECs into myofibroblasts inhibited by transfection of an siRNA against ALK5. (**a**–**f**) ECs transfected with an siRNA against ALK5 (siALK5) or a non-targeting siRNA (siCTRL), were incubated in the absence (−) or presence (+, 10 μM H_2O_2) of H_2O_2 for 72 h, and then protein expression was analyzed. (**a**, **c**, and **e**) Representative images from western blot experiments performed for detection of the endothelial marker VE-cadherin (VE-cad) (**a**), fibrotic marker α-SMA (**c**), and ECM proteins fibronectin (FN) (**e**). Panels (**b**, **d**, and **f**) show densitometric analyses from several experiments, as shown in (**a**, **c**, and **e**), respectively. Protein levels were normalized against tubulin, and the data are expressed relative to the untreated (0 μM H_2O_2 in siCTRL-transfected cells) condition. Statistical differences were assessed by a one-way analysis of variance (ANOVA) (Kruskal–Wallis) followed by Dunn's *post hoc* test. **: $P<0.01$ against the untreated (0 μM H_2O_2 in siCTRL-transfected cells) condition. NS: non-significant. Graph bars show the mean ± s.d. ($N=3$–4).

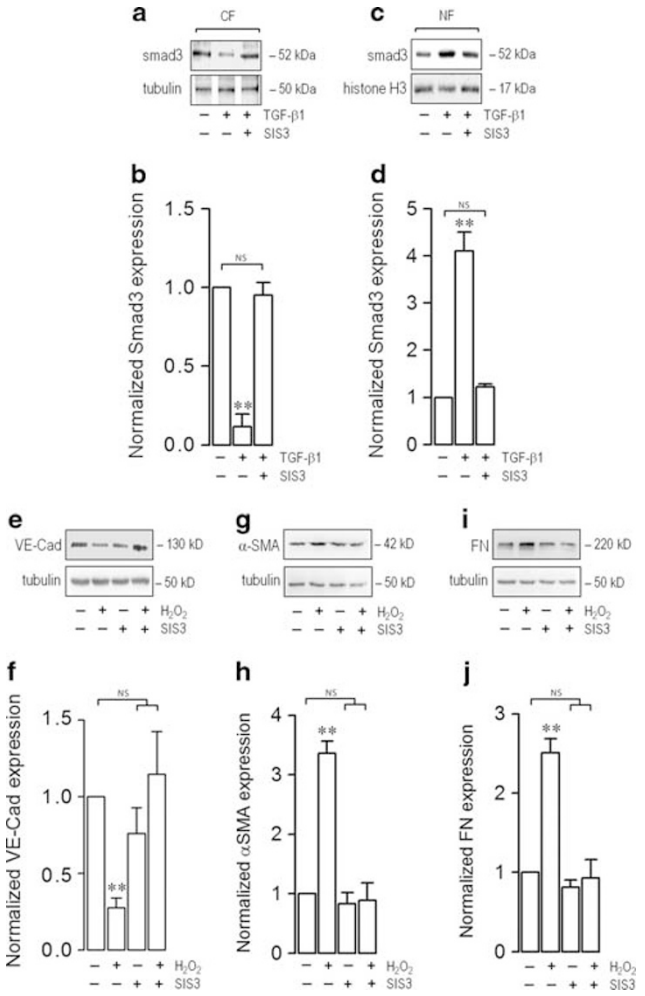

Figure 6 Changes in protein expression during H_2O_2-induced conversion of ECs into myofibroblasts inhibited by the specific inhibitor of Smad3, SIS3. (**a**–**d**) Cytosol (CF) and nuclear (NF) fractions were obtained from non-treated ECs and EC treated with TGF-β1 (10 ng/ml) in the presence or absence of 5 μM SIS3 for 72 h, and expression of smad3 was analyzed. (**a, c**) Representative images from western blot experiments performed for detection of smad3 in the CF (**a**) and NF (**c**) from non-treated ECs and EC treated with TGF-β1 in the presence or absence of SIS3. (**b** and **d**) Densitometric analyses of the experiments shown in (**a** and **c**), respectively. Protein levels were normalized against tubulin and histone H3 for CF and NF, respectively, and data are expressed relative to non-treated condition ($N=3$). (**e**–**j**) ECs were incubated in the absence (−) or presence (+) of 10 μM H_2O_2 for 72 h and treated in the absence (−) or presence (+) of 5 μM SIS3 for 72 h, and then protein expression was analyzed. (**e**, **g**, and **i**) Representative images from western blot experiments performed for detection of the endothelial marker VE-cadherin (VE-cad) (**e**), fibrotic marker α-SMA (**g**) and ECM proteins fibronectin (FN) (**i**). Panels (**f**, **h**, and **j**) show densitometric analyses from several experiments, as shown in (**e**, **g**, and **i**), respectively. Protein levels were normalized against tubulin, and the data are expressed relative to the untreated (0 μM H_2O_2 in the absence of SIS3) condition. Statistical differences were assessed by a one-way analysis of variance (ANOVA) (Kruskal–Wallis) followed by Dunn's *post hoc* test. **: $P<0.01$ against the untreated (0 μM H_2O_2 in the absence of SIS3) condition. NS: non-significant. Graph bars show the mean ± s.d. ($N=3$–4).

against TGF-β1 (siTGFβ1) showed a significant inhibition of TGF-β1 expression (Supplementary Figure S4a). Similarly, the siRNA against TGF-β2 (siTGFβ2) showed a significant inhibition of TGF-β2 expression (Supplementary Figure S4b). Of note, we observed that the action of siTGFβ1 also inhibited the expression of TGF-β2 (Supplementary Figure S4b). This finding was in accordance with previously reported data.[55] However, the action of siTGFβ2 did not affect the expression of TGF-β1 (Supplementary Figure S4a). Then, we tested whether the downregulation of TGF-β1 and TGF-β2 in the absence of any stimulus changed the protein levels of VE-cadherin, α-SMA, and fibronectin. As shown in Supplementary Figure S5a, ECs transfected with siTGFβ1 and siTGFβ2 showed a non-significant increase in the protein level of VE-cadherin and they showed a slight but significant decrease in the fibrotic protein α-SMA (Supplementary Figure S5b) and FN (Supplementary Figure S5c), suggesting that suppression of TGF-β1 and TGF-β2 expression did not promote any fibrotic processes.

Next, we determined whether the H_2O_2-induced conversion of ECs into myofibroblasts was dependent on TGF-β1

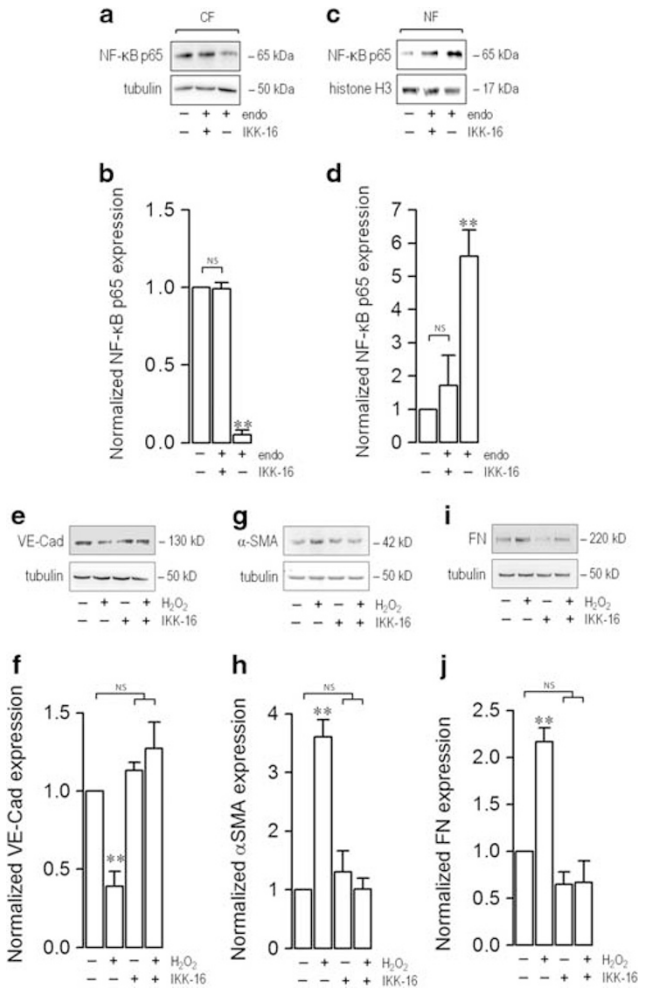

Figure 7 Changes in protein expression during H_2O_2-induced conversion of ECs into myofibroblasts inhibited by the specific inhibitor of NF-κB, IKK-16. (**a**–**d**) Cytosol (CF) and nuclear (NF) fractions were obtained from non-treated ECs and EC treated with endotoxin (10 μg/ml) in the presence or absence of 1 μM IKK-16 for 72 h, and expression of NF-κB p65 was analyzed. (**a, c**) Representative images from western blot experiments performed for detection of NF-κB p65 in the CF (**a**) and NF (**c**) from non-treated ECs and EC treated with endotoxin in the presence or absence of IKK-16. (**b** and **d**) Densitometric analyses of the experiments shown in (**a** and **c**), respectively. Protein levels were normalized against tubulin and histone H3 for CF and NF, respectively, and data are expressed relative to non-treated condition ($N = 3$). (**e**–**j**) ECs were incubated in the absence (−) or presence (+) of 10 μM H_2O_2 for 72 h and treated in the absence (−) or presence (+) of 1 μM IKK-16 for 72 h, and then protein expression was analyzed. (**e**, **g**, and **i**) Representative images from western blot experiments performed for detection of the endothelial marker VE-cadherin (VE-cad) (**e**), fibrotic marker α-SMA (**g**) and ECM proteins fibronectin (FN) (**i**). Panels (**f**, **h**, and **j**) show densitometric analyses from several experiments, as shown in (**e**, **g**, and **i**), respectively. Protein levels were normalized against tubulin, and the data are expressed relative to the untreated (0 μM H_2O_2 in the absence of IKK-16) condition. Statistical differences were assessed by a one-way analysis of variance (ANOVA) (Kruskal–Wallis) followed by Dunn's *post hoc* test. **: $P < 0.01$ against the untreated (0 μM H_2O_2 in the absence of IKK-16) condition. NS: non-significant. Graph bars show the mean ± s.d. ($N = 3$–4).

and TGF-β2 expression. ECs were transfected with siTGFβ1 or siTGFβ2, and endothelial and fibrotic markers were detected. ECs transfected with siCTRL and exposed to H_2O_2 exhibited a decrease in the protein level of the endothelial protein VE-cadherin (Figure 9a, b, g, and h) and an increase in the fibrotic markers α-SMA (Figure 9c, d, i, and j) and FN (Figure 9e, f, k, and l), which was similar to what was observed in non-transfected wild-type ECs, and denoted that a fibrotic process took place. Noteworthy, ECs transfected with siTGFβ1 or siTGFβ2 and exposed to H_2O_2 were resistant to fibrosis development because those cells did not show altered protein levels of endothelial (Figure 9a, b,, g, and h) or fibrotic markers (Figure 9c, f, i, and l). These results suggest that H_2O_2-induced conversion of ECs into myofibroblasts is dependent on TGF-β1 and TGF-β2 expression.

Afterward, we investigated the effect of TGF-β1 and TGF-β2 expression on the cellular localization and distribution of endothelial and fibrotic proteins. ECs transfected with siCTRL in the absence of H_2O_2 showed VE-cadherin (Figure 10a and c) and CD31 (Figure 10b and d) labeling that was localized at the plasma membrane. On the contrary, the expression of the fibrotic marker FSP-1 (Figure 10a) and α-SMA (Figure 10b) was weak, and the expression of the ECM protein fibronectin was slightly detected (Figure 10c and d), which was similar results to those observed in non-transfected wild-type ECs (Figures 2 and 4) that were depicted as a round-shape monolayer, short-spindle morphology with a cobblestone appearance. Similar results were obtained for ECs transfected with siTGFβ1 (Figure 10e–h) and siTGFβ2 (Figure 10i–l) in the absence of the oxidant. However, ECs transfected with siCTRL and exposed to H_2O_2 showed a decrease in the endothelial proteins VE-cadherin (Figure 10m and o) and CD31 (Figure 10n and p). Furthermore, H_2O_2 exposure induced an increase in the fibrotic markers FSP-1 (Figure 10m) and α-SMA (Figure 10n), as well as an increase in the expression of the ECM protein fibronectin (Figure 10o and p), thus resulting in a spindle-shaped, fibroblast-like phenotype that had lost cell-to-cell connections. Of note, ECs transfected with siTGFβ1 (Figure 10q–t) and siTGFβ2 (Figure 10u–y) and exposed to H_2O_2 were resistant to fibrosis progression. Transfected ECs did not exhibit changes in endothelial nor fibrotic markers, which confirmed that H_2O_2-induced conversion of ECs into myofibroblasts is dependent on TGF-β1 and TGF-β2 expression.

DISCUSSION

Endothelial dysfunction is a crucial factor in the development of systemic inflammation pathogenesis. Therefore, the study of the underlying cellular and molecular mechanisms that promote the dysfunction is fundamental for improving current therapies against systemic inflammation and developing new treatments.

It has been reported that the mediators of inflammation induce the conversion of ECs into myofibroblasts through an

EndMT pathway. The effect of TGF-β inducing the EndMT is well known.[34,35] In addition, tumor necrosis factor alpha (TNF-α), interleukin-6 (IL-6), and IL-1β also induce the EndMT.[41,56,57] Furthermore, we recently demonstrated that the endotoxin lipopolysaccharide induces the acquisition of fibrotic-like phenotype in ECs.[37] This conversion rises as a potential mechanism that begins endothelial dysfunction during the inflammatory process.

Because ROS generation is a hallmark of systemic inflammation due to mediators of inflammation eliciting an increment in ROS production, we focused on the capacity of ROS to promote conversion of ECs into myofibroblasts and investigated the underlying mechanism.

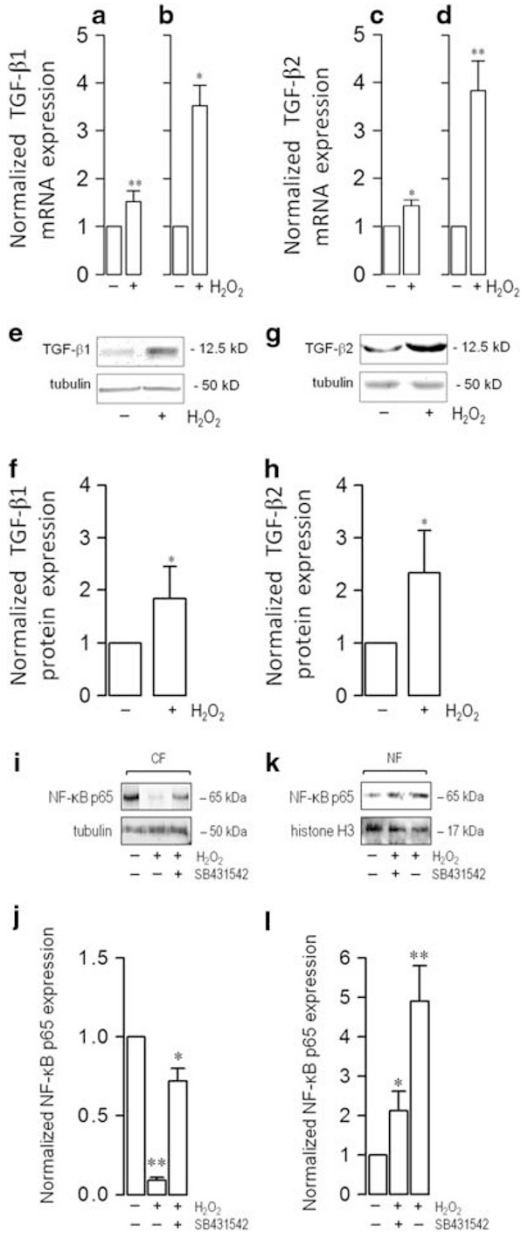

In this study, we demonstrated that H_2O_2 is able to induce conversion of ECs into myofibroblasts *via* an EndMT-like process. Our results show that H_2O_2 downregulates endothelial markers and upregulates fibroblast-specific and ECM proteins. Furthermore, we demonstrate that H_2O_2-induced conversion of ECs into myofibroblasts is mediated by a mechanism that depends on ALK5 expression, Smad3 activation, and NF-κB activity. Moreover, H_2O_2 induces the enhanced expression of TGF-β1 and TGF-β2, possibly by p38 MAPK phosphorylation. In addition, the downregulation of TGF-β1 and TGF-β2 abolished H_2O_2-induced conversion of ECs into myofibroblasts. Findings showed here were summarized in an integrative proposed model (Figure 11).

H_2O_2 exposure induces a change in the protein expression of endothelial and fibrotic markers. Decreased levels of endothelial adhesion proteins collaborate to allow cell-to-cell separation and generate the spindle-shaped, fibroblast-like phenotype, which is strongly potentiated by the overexpression of α-SMA stress fibers. As our results show, H_2O_2 challenge induced the overexpression of fibronectin and collagen type III. Healthy cells secrete ECM proteins in equilibrium with their degradation. During fibrosis, cells secrete high amounts of ECM proteins that overwhelm the cellular capacity for ECM degradation and generate morphological changes, as well as loss of cellular function.[44,45] Healthy ECs secrete low amounts of fibronectin and collagen type IV, while collagen type I and type III are nearly absent and appear only after fibrosis has been established.[44–47] We demonstrated that ECs exposed to oxidative stress

Figure 8 Oxidative stress induces the expression and secretion of TGF-β1 and TGF-β2. (**a**–**d**) ECs were incubated in the absence (−) or presence (+) of 10 μM H_2O_2 for 24 (**a**, **c**) or 72 h (**b**, **d**), and mRNA expression of TGF-β1 (**a, b**) and TGF-β2 (**c, d**) was then measured by means of qPCR. Determinations were performed in at least triplicates, and the results are expressed normalized relative to 28S mRNA expression. Significant differences were assessed by Student's *t*-test (Mann–Whitney). *, $P<0.05$, **, $P<0.01$ against untreated condition. Graph bars show the mean ± s.d. ($N=3$–5). (**e**–**h**) ECs were incubated in the absence (−) or presence (+) of 10 μM H_2O_2 for 72 h, and the protein secretion of TGF-β1 (**e**, **f**) and TGF-β2 (**g**, **h**) was then measured in the supernatant. (**e, g**) Representative images of western blot experiments performed for detection of TGF-β1 (**e**) and TGF-β2 (**g**) secretion. (**f** and **h**) Densitometric analyses of the experiments shown in (**e** and **g**), respectively. Protein levels were normalized against tubulin, and data are expressed relative to the untreated condition. Significant differences were assessed by Student's *t*-test (Mann–Whitney). *, $P<0.05$ and **, $P<0.01$ against untreated condition. Graph bars show the mean ± s.d. ($N=3$–4). (**i**–**l**) Cytosol (CF) and nuclear (NF) fractions were obtained from non-treated ECs and EC treated in the absence (−) or presence (+, 10 μM H_2O_2) of H_2O_2 for 72 h, with or without 0.5 μM SB431542 for 72 h, and expression of NF-κB p65 was analyzed. (**i**, **k**) Representative images from western blot experiments performed for detection of NF-κB p65 in the CF (**i**) and NF (**k**) from non-treated ECs and EC treated with H_2O_2 in the presence or absence of SB431542. (**j** and **l**) Densitometric analyses of the experiments shown in (**i** and **k**), respectively. Protein levels were normalized against tubulin and histone H3 for CF and NF, respectively, and data are expressed relative to non-treated condition ($N=3$).

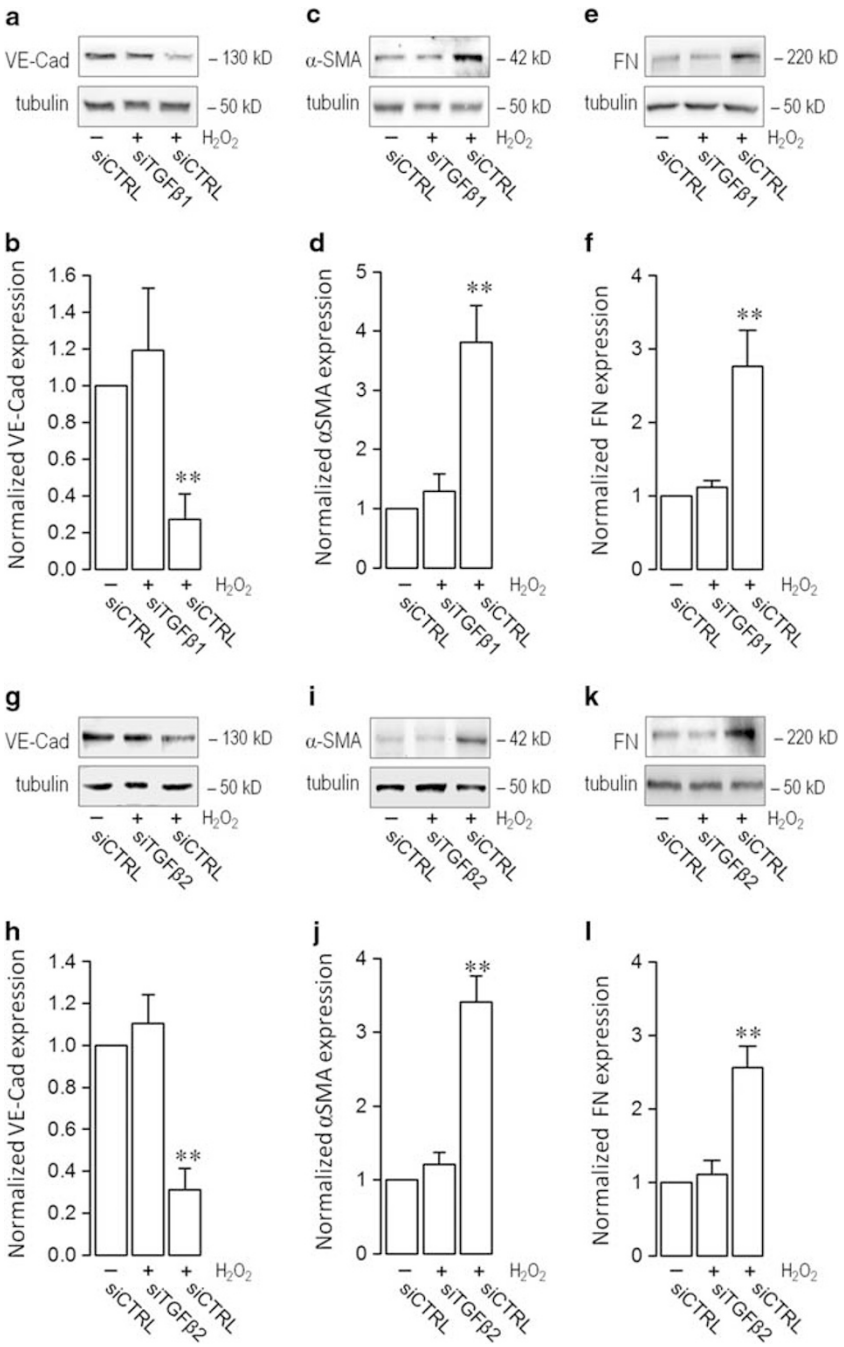

Figure 9 Changes in protein expression during H_2O_2-induced conversion of ECs into myofibroblasts inhibited by transfection of an siRNA against TGF-β1 and TGF-β2. (**a**–**l**) ECs transfected with an siRNA against TGF-β1 (siTGFβ1) (**a**–**f**), an siRNA against TGF-β2 (siTGFβ2) (**g**–**l**) or a non-targeting siRNA (siCTRL) (**a**–**l**), and incubated in the absence (−) or presence (+) of 10 μM H_2O_2 for 72 h, and then protein expression was analyzed. (**a**, **c**, **e**, **g**, **i,** and **k**) Representative images from western blot experiments performed for detection of the endothelial marker VE-cadherin (VE-cad) (**a**, **g**), fibrotic marker α-SMA (**c, i**) and ECM proteins fibronectin (FN) (**e, k**). Panels (**b**, **d**, **f**, **h**, **j,** and **f**) show densitometric analyses from several experiments, as shown in (**a**, **c**, **e**, **g**, **i** and **k**), respectively. Protein levels were normalized against tubulin, and the data are expressed relative to the siCTRL-transfected cells condition in the absence of H_2O_2. Statistical differences were assessed by a one-way analysis of variance (ANOVA) (Kruskal–Wallis) followed by Dunn's *post hoc* test. **: $P<0.01$ against the siCTRL-transfected cells condition in the absence of H_2O_2. Graph bars show the mean ± s.d. ($N=3$–4).

overexpress the ECM proteins fibronectin and collagen type III, suggesting that oxidative stress induces abnormal ECM overload in ECs. Because ECM proteins are molecular bridges by which bacteria adhere and invade host cells, the oxidative stress-induced ECM overexpression could represent a mechanism to generate bacterial pathogenesis and enhance the inflammatory response. Certainly, further studies are needed to test this idea.

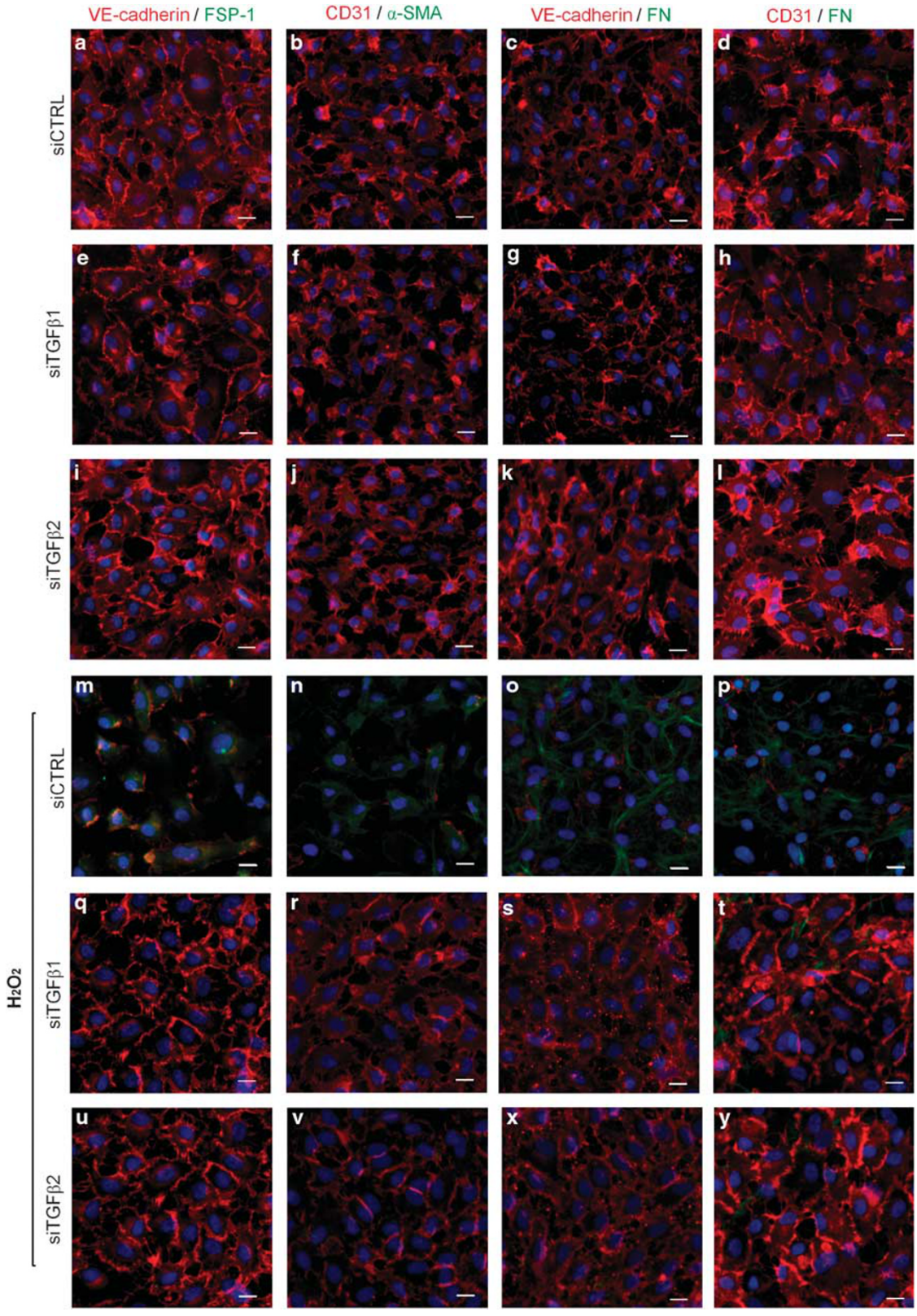

Figure 10 Cellular distribution of endothelial and fibrotic markers involved in H_2O_2-induced conversion of ECs into myofibroblasts inhibited by transfection of an siRNA against TGF-β1 and TGF-β2. (**a**–**y**) Representative images from ECs transfected with an siRNA against TGF-β1 (siTGFβ1) (**e**–**h** and **q**–**t**), an siRNA against TGF-β2 (siTGFβ2) (**i**–**l** and **u**–**y**) or a non-targeting siRNA (siCTRL) (**a**–**d** and **m**–**p**), and incubated in the absence ($-$) or presence ($+$) of 10 μM H_2O_2 for 72 h. VE-cadherin or CD31 (red), and FSP-1, α-SMA, or FN (green) were detected. Nuclei were stained using DAPI. Bar scale represents 10 μm ($N = 3$).

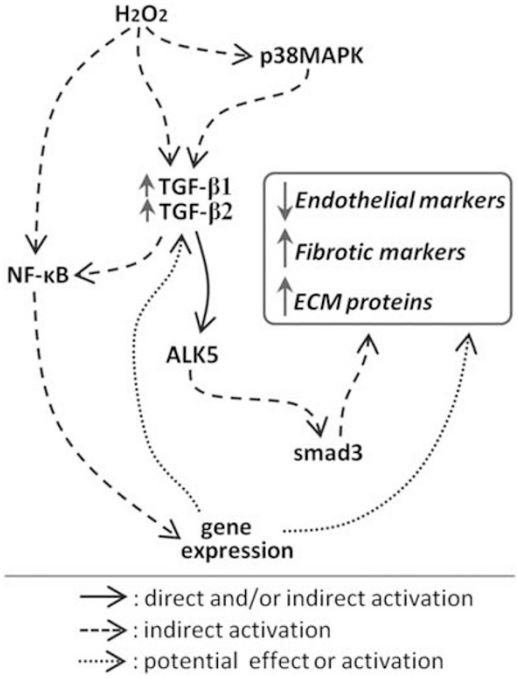

Figure 11 Proposed model of H_2O_2-induced conversion of ECs into myofibroblasts *via* a TGF-β1 and TGF-β2-dependent pathway. (i) We demonstrated that H_2O_2 induces the conversion of ECs into myofibroblasts, changing the expression of endothelial markers, fibrotic markers, and ECM proteins. (ii) It has been widely demonstrated that H_2O_2 activates NF-κB to induce gene expression.[62–66] This gene expression could be involved in the H_2O_2-induced conversion of ECs into myofibroblasts because inhibition of NF-κB using IKK-16 inhibited the conversion. (iii) Our results showed that H_2O_2 induces the phosphorylation of p38MAPK. It is well known that p38MAPK activation induces TGF-β1 and TGF-β2 production.[6,24] (iv) TGF-β activates the receptor ALK5, eliciting the Smad protein intracellular pathway. Smad3 activation contributes to the induction of gene expression and the promotion of fibrosis.[24,29,30,74,75,77] Some data suggest that Smad3 can be activated by H_2O_2.[78,79] (v) It has been clearly demonstrated that the action of TGF-β is induced through the activation of NF-κB.[25,26,75,76,80,81] At the same time, it has been reported that NF-κB activation induces TGF-β production.[82–84] Thus, there is a potential positive feedback mechanism between TGF-β production and NF-κB activation that enhances the fibrotic process. (vi) Furthermore, we used RT-qPCR and protein detection by western blot to demonstrate that H_2O_2 induces the expression and secretion of TGF-β1 and TGF-β2, and it has been clearly demonstrated that TGF-β1 and TGF-β2 induce the conversion of ECs into myofibroblasts.[19,34,35,40,41,85]

Our findings showing that oxidative stress is able to generate conversion of ECs into myofibroblasts through an EndMT-like mechanism are in accordance with evidence showing that ROS stimulate the EMT in renal cells and keratinocytes.[31,32] In contrast, it was recently reported that ROS production inhibits the EMT in prostate cancer cells.[58] Because the EndMT is also observed in tumor cells, it would be interesting to explore whether oxidative stress inhibits the EndMT in cancer cells.

During systemic inflammation, the activated cells of the immune system, including macrophages and phagocytes, oversecrete a number of oxidative molecules. These reactive molecules are generated in organs and interact with several cells to modify their activity. In the vascular system, the oxidative molecules circulating in blood vessels inevitably interact with ECs. Thus, the intracellular level of ROS in ECs is greatly elevated.[1,9] H_2O_2 and other oxidant molecules can upregulate or downregulate several proteins, such as the protooncogenes c-jun, c-fos, and c-myc,[12] the TRPM7 calcium channel,[13] cyclooxygenase-2 and prostaglandins,[14] and the intercellular adhesion molecule-1 (ICAM-1) and vascular cell adhesion molecule-1 (VCAM-1),[15] which promotes changes in several cellular functions. Moreover, the actions of oxidative stress on gene expression are mainly mediated by activating transcription factors such as NF-κB, activator protein-1 (AP-1) and the JAK-STAT pathway.[59–61] In fact, it has been widely reported that NF-κB is activated by H_2O_2 and other oxidants.[62–66] In the present study, we demonstrated that H_2O_2 mediates its action through the ALK5/Smad3/NF-κB intracellular pathway. These findings suggest possibly that the NF-κB transcription factor is involved in the modification of protein expression that is induced by oxidative stress.

On the other hand, oxidative stress can modify proteins such as kinases, phosphatases, ion channels, transcriptional factors, and receptors.[7,67–72] Thus, ameliorating oxidative stress-induced conversion of ECs into myofibroblasts with antioxidants and reducing agents could be useful for treatment.

The dependence of ALK5 activity on H_2O_2-induced conversion of ECs into myofibroblasts indicates that its ligand, TFG-β, should be involved in this process. We show here that H_2O_2 increases TGF-β1 and TGF-β2 expression. Moreover, the H_2O_2-induced p38 MAPK phosphorylation indicates a possible mechanism for the increased expression of TGF-β1 and TGF-β2. In addition to the role played by activated p38 MAPK in enhancing TGF-β expression, TGF-β intracellular signaling is mediated *via* p38 MAPK phosphorylation.[73,74] Thus, it would be interesting to test whether H_2O_2-induced conversion of ECs into myofibroblasts is inhibited by a p38 MAPK inhibitor; however, further experiments are needed to test this idea. Although NF-κB activity is normally suppressed by TGF-β in normal cells, NF-κB can be activated upon TGF-β treatment in pathological cells,[25,26,75,76] which could be the mechanism for H_2O_2-induced conversion of ECs into myofibroblasts.

Considering the results showed here, and the literature regarding these issues, if the H_2O_2-induced conversion of ECs into myofibroblasts is mediated by TGF-β1 or TGF-β2 production, is reasonable to assume that fibrotic changes might appear earlier when ECs are directly stimulated by TGF-β; however, when ECs are treated with the oxidant, the fibrosis became visible at a later time point.

Taken together, the results shown here provide evidence that oxidative stress is a crucial factor in inducing the conversion of ECs into myofibroblasts through a TGF-β-dependent mechanism that produces changes in EC protein

expression by converting them from normal to pathological. This information will be useful in designing new and improved therapeutic strategies against oxidative stress-mediated systemic inflammatory diseases.

Supplementary Information accompanies the paper on the Laboratory Investigation website (http://www.laboratoryinvestigation.org)

ACKNOWLEDGMENTS

This work was supported by research grants from Fondo Nacional de Desarrollo Científico y Tecnológico - Fondecyt 1121078 (FS), 1120380 (CCV), 1120976 (RF), 3140448 (CE), 3130593 (MGM), Millennium Institute on Immunology and Immunotherapy P09-016-F (FS), Association-Francaise Contre Les Myopathies AFM 16670 (CCV), UNAB-DI-281-13/R (CCV), and UNAB-DI-67-12/I (CE). We are grateful to Director Dr Iván Oyarzún and Dr Mario Carmona, Dr Jaime Mendoza, and Mrs. Juana Belmar from Servicio Ginecología y Obstetricia, Hospital San Jose de Melipilla.

DISCLOSURE/CONFLICT OF INTEREST

The authors declare no conflict of interest.

1. Closa D, Folch-Puy E. Oxygen free radicals and the systemic inflammatory response. IUBMB Life 2004;56:185–191.
2. Nagata M. Inflammatory cells and oxygen radicals. Curr Drug Targets Inflamm Allergy 2005;4:503–504.
3. Cai H, Harrison DG. Endothelial dysfunction in cardiovascular diseases: the role of oxidant stress. Circ Res 2000;87:840–844.
4. Droge W. Free radicals in the physiological control of cell function. Physiol Rev 2002;82:47–95.
5. Bryan N, Ahswin H, Smart N, *et al.* Reactive oxygen species (ROS)–a family of fate deciding molecules pivotal in constructive inflammation and wound healing. Eur Cell Mater 2012;24:249–265.
6. Morales MG, Vazquez Y, Acuna MJ, *et al.* Angiotensin II-induced pro-fibrotic effects require p38MAPK activity and transforming growth factor beta 1 expression in skeletal muscle cells. Int J Biochem Cell Biol 2012;44:1993–2002.
7. Cabello-Verrugio C, Acuna MJ, Morales MG, *et al.* Fibrotic response induced by angiotensin-II requires NAD(P)H oxidase-induced reactive oxygen species (ROS) in skeletal muscle cells. Biochem Biophys Res Commun 2011;410:665–670.
8. Simon F, Fernandez R. Early lipopolysaccharide-induced reactive oxygen species production evokes necrotic cell death in human umbilical vein endothelial cells. J Hypertens 2009;27:1202–1216.
9. Muller MM, Griesmacher A. Markers of endothelial dysfunction. Clin Chem Lab Med 2000;38:77–85.
10. Griendling KK, Sorescu D, Lassegue B, *et al.* Modulation of protein kinase activity and gene expression by reactive oxygen species and their role in vascular physiology and pathophysiology. Arterioscler Thromb Vasc Biol 2000;20:2175–2183.
11. Antonelou MH, Kriebardis AG, Velentzas AD, *et al.* Oxidative stress-associated shape transformation and membrane proteome remodeling in erythrocytes of end stage renal disease patients on hemodialysis. J Proteomics 2011;74:2441–2452.
12. Li DW, Spector A. Hydrogen peroxide-induced expression of the proto-oncogenes, c-jun, c-fos and c-myc in rabbit lens epithelial cells. Mol Cell Biochem 1997;173:59–69.
13. Nunez-Villena F, Becerra A, Echeverria C, *et al.* Increased expression of the transient receptor potential melastatin 7 channel is critically involved in lipopolysaccharide-induced reactive oxygen species-mediated neuronal death. Antioxid Redox Signal 2011;15:2425–2438.
14. Kiritoshi S, Nishikawa T, Sonoda K, *et al.* Reactive oxygen species from mitochondria induce cyclooxygenase-2 gene expression in human mesangial cells: potential role in diabetic nephropathy. Diabetes 2003;52:2570–2577.
15. Roebuck KA, Rahman A, Lakshminarayanan V, *et al.* H2O2 and tumor necrosis factor-alpha activate intercellular adhesion molecule 1 (ICAM-1) gene transcription through distinct cis-regulatory elements within the ICAM-1 promoter. J Biol Chem 1995;270:18966–18974.
16. Sihvo EI, Salminen JT, Rantanen TK, *et al.* Oxidative stress has a role in malignant transformation in Barrett's oesophagus. Int J Cancer 2002; 102:551–555.
17. Behrend L, Henderson G, Zwacka RM. Reactive oxygen species in oncogenic transformation. Biochem Soc Trans 2003;31:1441–1444.
18. Uziel O, Reshef H, Ravid A, *et al.* Oxidative stress causes telomere damage in Fanconi anaemia cells - a possible predisposition for malignant transformation. Br J Haematol 2008;142:82–93.
19. Medici D, Potenta S, Kalluri R. Transforming growth factor-beta2 promotes Snail-mediated endothelial-mesenchymal transition through convergence of Smad-dependent and Smad-independent signalling. Biochem J 2011;437:515–520.
20. Ishisaki A, Hayashi H, Li AJ, *et al.* Human umbilical vein endothelium-derived cells retain potential to differentiate into smooth muscle-like cells. J Biol Chem 2003;278:1303–1309.
21. Krenning G, Moonen JR, van Luyn MJ, *et al.* Vascular smooth muscle cells for use in vascular tissue engineering obtained by endothelial-to-mesenchymal transdifferentiation (EnMT) on collagen matrices. Biomaterials 2008;29:3703–3711.
22. Moonen JR, Krenning G, Brinker MG, *et al.* Endothelial progenitor cells give rise to pro-angiogenic smooth muscle-like progeny. Cardiovasc Res 2010;86:506–515.
23. Lebrin F, Deckers M, Bertolino P, *et al.* TGF-beta receptor function in the endothelium. Cardiovasc Res 2005;65:599–608.
24. Santibanez JF, Quintanilla M, Bernabeu C. TGF-beta/TGF-beta receptor system and its role in physiological and pathological conditions. Clin Sci (Lond) 2011;121:233–251.
25. Freudlsperger C, Bian Y, Contag WS, *et al.* TGF-beta and NF-kappaB signal pathway cross-talk is mediated through TAK1 and SMAD7 in a subset of head and neck cancers. Oncogene 2013;32:1549–1559.
26. Ishinaga H, Jono H, Lim JH, *et al.* Synergistic induction of nuclear factor-kappaB by transforming growth factor-beta and tumour necrosis factor-alpha is mediated by protein kinase A-dependent RelA acetylation. Biochem J 2009;417:583–591.
27. Habashi JP, Doyle JJ, Holm TM, *et al.* Angiotensin II type 2 receptor signaling attenuates aortic aneurysm in mice through ERK antagonism. Science 2011;332:361–365.
28. Holm TM, Habashi JP, Doyle JJ, *et al.* Noncanonical TGFbeta signaling contributes to aortic aneurysm progression in Marfan syndrome mice. Science 2011;332:358–361.
29. Gauldie J, Bonniaud P, Sime P, *et al.* TGF-beta, Smad3 and the process of progressive fibrosis. Biochem Soc Trans 2007;35:661–664.
30. Gauldie J, Kolb M, Ask K, *et al.* Smad3 signaling involved in pulmonary fibrosis and emphysema. Proc Am Thorac Soc 2006;3:696–702.
31. Fukawa T, Kajiya H, Ozeki S, *et al.* Reactive oxygen species stimulates epithelial mesenchymal transition in normal human epidermal keratinocytes *via* TGF-beta secretion. Exp Cell Res 2012;318:1926–1932.
32. Rhyu DY, Yang Y, Ha H, *et al.* Role of reactive oxygen species in TGF-beta1-induced mitogen-activated protein kinase activation and epithelial-mesenchymal transition in renal tubular epithelial cells. J Am Soc Nephrol 2005;16:667–675.
33. Ding SZ, Yang YX, Li XL, *et al.* Epithelial-mesenchymal transition during oncogenic transformation induced by hexavalent chromium involves reactive oxygen species-dependent mechanism in lung epithelial cells. Toxicol Appl Pharmacol 2013;269:61–71.
34. Potenta S, Zeisberg E, Kalluri R. The role of endothelial-to-mesenchymal transition in cancer progression. Br J Cancer 2008;99: 1375–1379.
35. Zeisberg EM, Potenta S, Xie L, *et al.* Discovery of endothelial to mesenchymal transition as a source for carcinoma-associated fibroblasts. Cancer Res 2007;67:10123–10128.
36. Echeverria C, Montorfano I, Hermosilla T, *et al.* Endotoxin induces fibrosis in vascular endothelial cells through a mechanism dependent on transient receptor protein melastatin 7 activity. PLoS ONE 2014; 9:e94146.
37. Echeverria C, Montorfano I, Sarmiento D, *et al.* Lipopolysaccharide induces a fibrotic-like phenotype in endothelial cells. J Cell Mol Med 2013;17:800–814.
38. Krenning G, Zeisberg EM, Kalluri R. The origin of fibroblasts and mechanism of cardiac fibrosis. J Cell Physiol 2010;225:631–637.
39. Hertig A, Gangadhar T, Kalluri R. Renal studies provide an insight into cardiac extracellular matrix remodeling during health and disease. J Mol Cell Cardiol 2010;48:497–503.

40. Maleszewska M, Moonen JR, Huijkman N, *et al.* IL-1beta and TGFbeta2 synergistically induce endothelial to mesenchymal transition in an NFkappaB-dependent manner. Immunobiology 2012;218:443–454.
41. Mahler GJ, Farrar EJ, Butcher JT. Inflammatory cytokines promote mesenchymal transformation in embryonic and adult valve endothelial cells. Arterioscler Thromb Vasc Biol 2013;33:121–130.
42. Ghosh AK, Nagpal V, Covington JW, *et al.* Molecular basis of cardiac endothelial-to-mesenchymal transition (EndMT): differential expression of microRNAs during EndMT. Cell Signal 2012;24:1031–1036.
43. Zhao L, Yang R, Cheng L, *et al.* LPS-induced epithelial-mesenchymal transition of intrahepatic biliary epithelial cells. J Surg Res 2010;171:819–825.
44. Sorokin L. The impact of the extracellular matrix on inflammation. Nat Rev Immunol 2010;10:712–723.
45. Wynn TA. Cellular and molecular mechanisms of fibrosis. J Pathol 2008;214:199–210.
46. Davis GE, Senger DR. Endothelial extracellular matrix: biosynthesis, remodeling, and functions during vascular morphogenesis and neovessel stabilization. Circ Res 2005;97:1093–1107.
47. Yurchenco PD, Amenta PS, Patton BL. Basement membrane assembly, stability and activities observed through a developmental lens. Matrix Biol 2004;22:521–538.
48. Thiery JP, Acloque H, Huang RY, *et al.* Epithelial-mesenchymal transitions in development and disease. Cell 2009;139:871–890.
49. Goumans MJ, van Zonneveld AJ, Ten Dijke P. Transforming growth factor beta-induced endothelial-to-mesenchymal transition: a switch to cardiac fibrosis? Trends Cardiovasc Med 2008;18:293–298.
50. Lappas M. Anti-inflammatory properties of sirtuin 6 in human umbilical vein endothelial cells. Mediators Inflamm 2012;2012:597514.
51. Dauphinee SM, Clayton A, Hussainkhel A, *et al.* SASH1 is a scaffold molecule in endothelial TLR4 signaling. J Immunol 2013;191:892–901.
52. Sarmiento D, Montorfano I, Cerda O, *et al.* Increases in reactive oxygen species enhance vascular endothelial cell migration through a mechanism dependent on the transient receptor potential melastatin 4 ion channel. Microvasc Res 2014;S0026-2862:00032–00036.
53. Cabello-Verrugio C, Morales MG, Cabrera D, *et al.* Angiotensin II receptor type 1 blockade decreases CTGF/CCN2-mediated damage and fibrosis in normal and dystrophic skeletal muscles. J Cell Mol Med 2012;16:752–764.
54. Jinnin M, Ihn H, Tamaki K. Characterization of SIS3, a novel specific inhibitor of Smad3, and its effect on transforming growth factor-beta1-induced extracellular matrix expression. Mol Pharmacol 2006;69:597–607.
55. Oh S, Kim E, Kang D, *et al.* Transforming growth factor-beta gene silencing using adenovirus expressing TGF-beta1 or TGF-beta2 shRNA. Cancer Gene Ther 2013;20:94–100.
56. Rieder F, Kessler SP, West GA, *et al.* Inflammation-induced endothelial-to-mesenchymal transition: a novel mechanism of intestinal fibrosis. Am J Pathol 2011;179:2660–2673.
57. Kanaji N, Sato T, Nelson A, *et al.* Inflammatory cytokines regulate endothelial cell survival and tissue repair functions *via* NF-kappaB signaling. J Inflamm Res 2011;4:127–138.
58. Das TP, Suman S, Damodaran C. Reactive oxygen species generation inhibits epithelial-mesenchymal transition and promotes growth arrest in prostate cancer cells. Mol Carcinog 2013;53:537–547.
59. Schreck R, Rieber P, Baeuerle PA. Reactive oxygen intermediates as apparently widely used messengers in the activation of the NF-kappa B transcription factor and HIV-1. EMBO J 1991;10:2247–2258.
60. Stauble B, Boscoboinik D, Tasinato A, *et al.* Modulation of activator protein-1 (AP-1) transcription factor and protein kinase C by hydrogen peroxide and D-alpha-tocopherol in vascular smooth muscle cells. Eur J Biochem 1994;226:393–402.
61. Simon AR, Rai U, Fanburg BL, *et al.* Activation of the JAK-STAT pathway by reactive oxygen species. Am J Physiol 1998;275:C1640–C1652.
62. Asehnoune K, Strassheim D, Mitra S, *et al.* Involvement of reactive oxygen species in Toll-like receptor 4-dependent activation of NF-kappa B. J Immunol 2004;172:2522–2529.
63. Satriano J, Schlondorff D. Activation and attenuation of transcription factor NF-kB in mouse glomerular mesangial cells in response to tumor necrosis factor-alpha, immunoglobulin G, and adenosine 3′:5′-cyclic monophosphate. Evidence for involvement of reactive oxygen species. J Clin Invest 1994;94:1629–1636.
64. Kim KJ, Cho KD, Jang KY, *et al.* Platelet-activating factor enhances tumor metastasis *via* the ROS-dependent protein kinase CK2-mediated NF-kappaB activation. Immunology 2014.
65. Kastl L, Sauer SW, Ruppert T, *et al.* TNF-alpha mediates mitochondrial uncoupling and enhances ROS-dependent cell migration *via* NF-kappaB activation in liver cells. FEBS Lett 2014;588:175–183.
66. Simard JC, Cesaro A, Chapeton-Montes J, *et al.* S100A8 and S100A9 induce cytokine expression and regulate the NLRP3 inflammasome *via* ROS-dependent activation of NF-kappaB(1.). PLoS ONE 2013;8:e72138.
67. Simon F, Leiva-Salcedo E, Armisen R, *et al.* Hydrogen peroxide removes TRPM4 current desensitization conferring increased vulnerability to necrotic cell death. J Biol Chem 2010;285:37150–37158.
68. Simon F, Varela D, Eguiguren AL, *et al.* Hydroxyl radical activation of a Ca(2+)-sensitive nonselective cation channel involved in epithelial cell necrosis. Am J Physiol Cell Physiol 2004;287:C963–C970.
69. Simon F, Varela D, Riveros A, *et al.* Non-selective cation channels and oxidative stress-induced cell swelling. Biol Res 2002;35:215–222.
70. Varela D, Simon F, Riveros A, *et al.* NAD(P)H oxidase-derived H(2)O(2) signals chloride channel activation in cell volume regulation and cell proliferation. J Biol Chem 2004;279:13301–13304.
71. Simon F, Varela D, Cabello-Verrugio C. Oxidative stress-modulated TRPM ion channels in cell dysfunction and pathological conditions in humans. Cell Signal 2013;25:1614–1624.
72. Becerra A, Echeverria C, Varela D, *et al.* Transient receptor potential melastatin 4 inhibition prevents lipopolysaccharide-induced endothelial cell death. Cardiovasc Res 2011;91:677–684.
73. Chin BY, Mohsenin A, Li SX, *et al.* Stimulation of pro-alpha(1)(I) collagen by TGF-beta(1) in mesangial cells: role of the p38 MAPK pathway. Am J Physiol Renal Physiol 2001;280:F495–F504.
74. Yu L, Hebert MC, Zhang YE. TGF-beta receptor-activated p38 MAP kinase mediates Smad-independent TGF-beta responses. EMBO J 2002;21:3749–3759.
75. Park JI, Lee MG, Cho K, *et al.* Transforming growth factor-beta1 activates interleukin-6 expression in prostate cancer cells through the synergistic collaboration of the Smad2, p38-NF-kappaB, JNK, and Ras signaling pathways. Oncogene 2003;22:4314–4332.
76. Neil JR, Schiemann WP. Altered TAB1:I kappaB kinase interaction promotes transforming growth factor beta-mediated nuclear factor-kappaB activation during breast cancer progression. Cancer Res 2008;68:1462–1470.
77. Derynck R, Zhang YE. Smad-dependent and Smad-independent pathways in TGF-beta family signalling. Nature 2003;425:577–584.
78. Li H, Sekine M, Seng S, *et al.* BRCA1 interacts with Smad3 and regulates Smad3-mediated TGF-beta signaling during oxidative stress responses. PLoS ONE 2009;4:e7091.
79. Choi J, Park SJ, Jo EJ, *et al.* Hydrogen peroxide inhibits transforming growth factor-beta1-induced cell cycle arrest by promoting Smad3 linker phosphorylation through activation of Akt-ERK1/2-linked signaling pathway. Biochem Biophys Res Commun 2013;435:634–639.
80. Ishinaga H, Jono H, Lim JH, *et al.* TGF-beta induces p65 acetylation to enhance bacteria-induced NF-kappaB activation. EMBO J 2007;26:1150–1162.
81. Chow JY, Ban M, Wu HL, *et al.* TGF-beta downregulates PTEN *via* activation of NF-kappaB in pancreatic cancer cells. Am J Physiol Gastrointest Liver Physiol 2010;298:G275–G282.
82. Ohga S, Shikata K, Yozai K, *et al.* Thiazolidinedione ameliorates renal injury in experimental diabetic rats through anti-inflammatory effects mediated by inhibition of NF-kappaB activation. Am J Physiol Renal Physiol 2007;292:F1141–F1150.
83. Yang J, Zeng Z, Wu T, *et al.* Emodin attenuates high glucose-induced TGF-beta1 and fibronectin expression in mesangial cells through inhibition of NF-kappaB pathway. Exp Cell Res 2013;319:3182–3189.
84. Wang L, Zhang D, Zheng J, *et al.* Actin cytoskeleton-dependent pathways for ADMA-induced NF-kappaB activation and TGF-beta high expression in human renal glomerular endothelial cells. Acta Biochim Biophys Sin (Shanghai) 2012;44:918–923.
85. Zeisberg EM, Tarnavski O, Zeisberg M, *et al.* Endothelial-to-mesenchymal transition contributes to cardiac fibrosis. Nat Med 2007;13:952–961.